FE/CU(100) ML=5.0

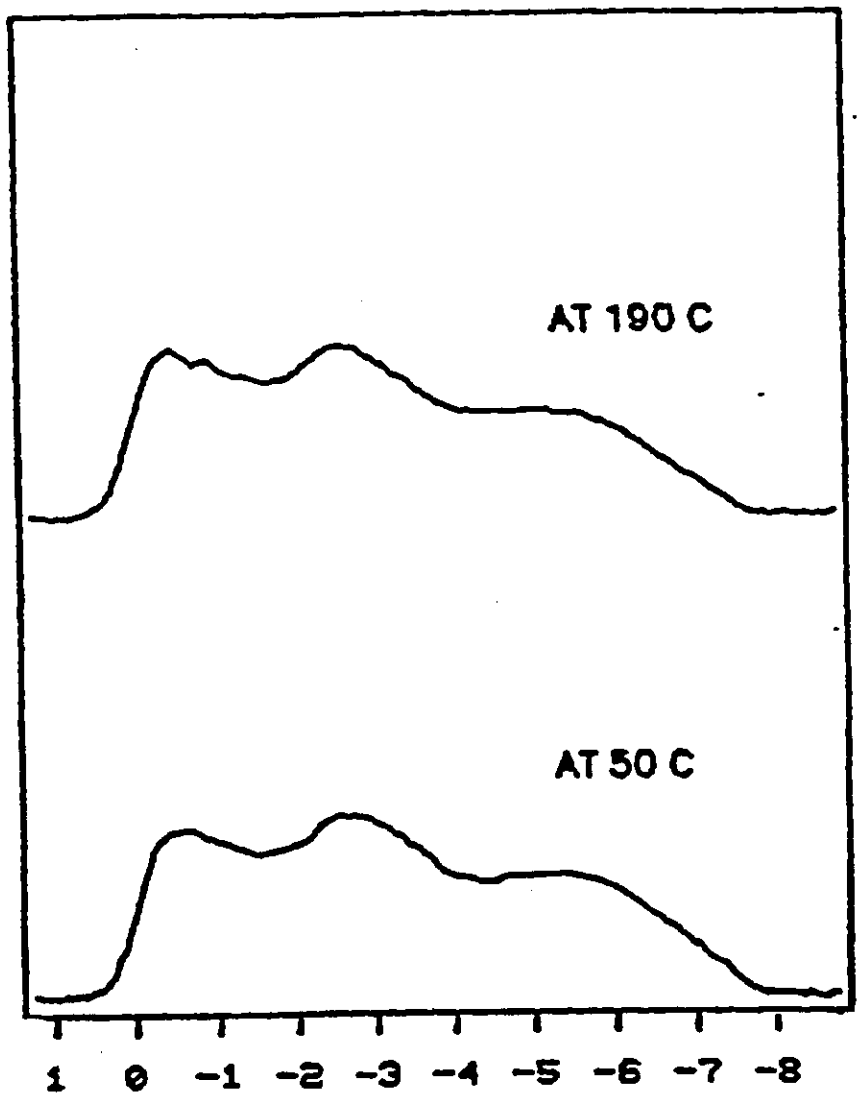

Fig. 4

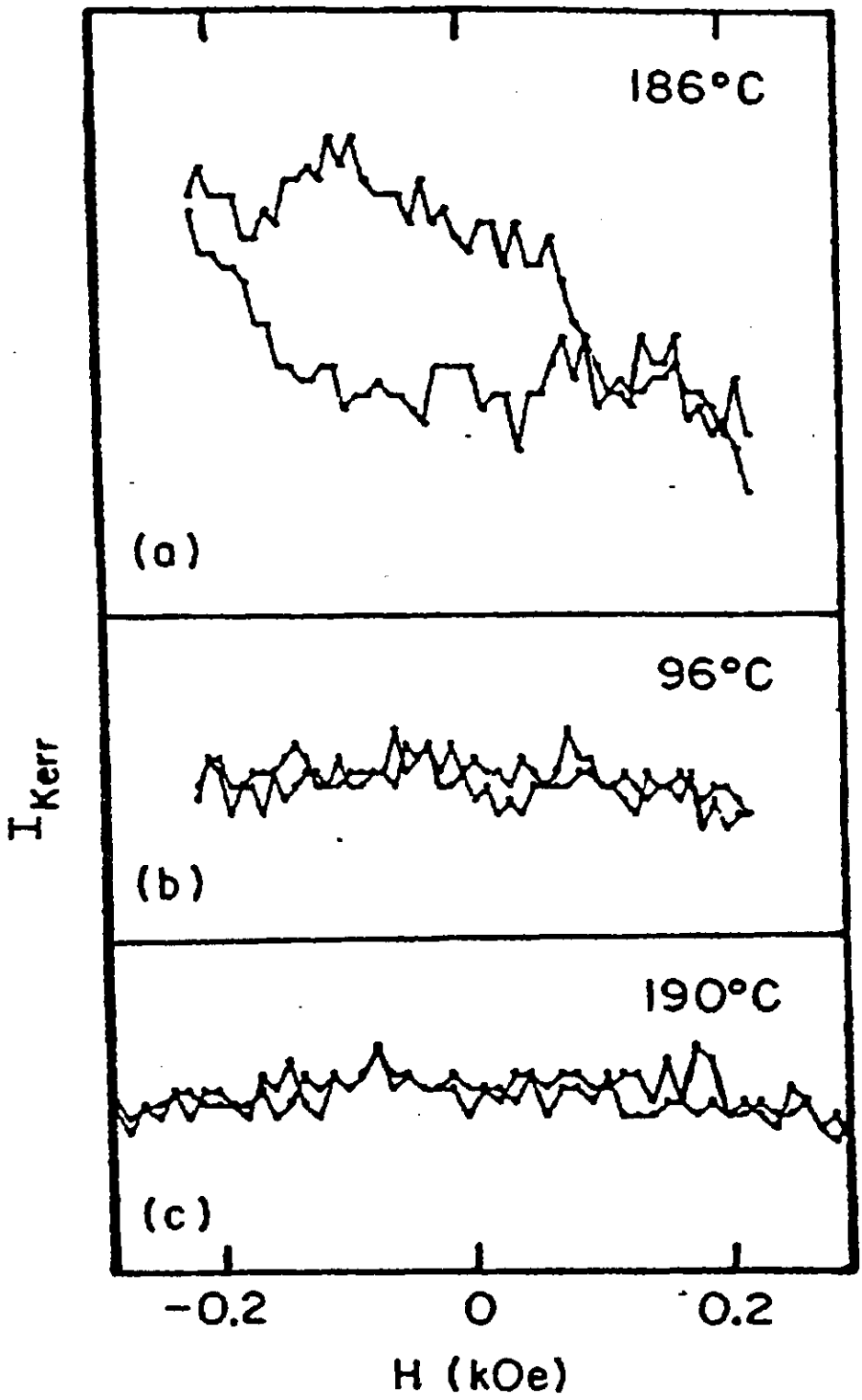

Fig. 5

5. TWO MAGNETICALLY-DIFFERENT CLOSELY LYING STATES OF Fcc IRON GROWN ON COPPER (100)

(Quarterly Report October 16, 1986 - January 15, 1987)

ABSTRACT

Two closely lying (in energy) states of fcc iron grown on copper (100) have been identified by magneto-optic and photoemission experiments. The as-grown state at 460K exhibits in-plane surface ferromagnetism in magneto-optic measurements. Ferromagnetism parallel to the plane is not observed for the room-temperature state; its absence is supported by a comparison of our calculated and measured work functions and by the photoemission results. LEED shows expanded interplanar spacing at the surface. The temperature behavior and effect of fresh iron deposition indicate that the thermal transition between the two states is first-order.

Understanding the mechanisms that select the crystal structures of the elements is one of the fundamental questions of solid state physics. This is especially interesting for iron because of the question of the "competition" between bcc and fcc structures and the role of magnetism in this competition. The ability[1,2] to prepare fcc iron films by epitaxial growth on copper has provided the opportunity to study directly the electronic structure of fcc iron.[3-5] Interestingly, quite conflicting conclusions have been reached as to the magnetic state of fcc iron grown on Cu(100).[3,4]

We have identified and characterized two closely lying (in energy) states of fcc iron grown on copper (100). One state (State L) has no ferromagnetism parallel to the surface and occurs at room temperature. The documentation for the nature of state L consists of the observations that the surface magneto-optic Kerr effect[6] (SMOKE) gives vanishing intensity (no hysteresis characteristic of ferromagnetism parallel to the surface), and the work function increases relative to Cu. The work function increase shows the same trend as that predicted by our self-consistent electronic structure calculations for paramagnetic fcc iron relative to Cu or bcc Fe or magnetically-ordered fcc Fe. The second state (State H) is ferromagnetic and occurs when the sample is kept at its growth temperature (420-460K); however, the experimental behavior indicates that the ferromagnetism is confined to the surface layer. This is consistent with our spin-polarized electronic structure calculations indicating the existence of a magnetically-ordered state with ferromagnetism at the surface, but antiferromagnetism in the interior. The documentation for the ferromagnetic nature of State H consists (a) of a significant SMOKE intensity (hysteresis) identifying ferromagnetism parallel to the surface at 460K, (b) a decreased work function compared to State L, consistent with the calculated trend predicted for magnetically-ordered as compared to paramag-

netic, fcc iron, (c) an indication of the presence of exchange splitting shown in the UPS behavior at 460K, . Below we give a detailed description of this study and relate our results to those of other workers.

The absence of ferromagnetism parallel to the surface at room temperature was definitively recognized by the absence of any SMOKE intensity throughout the thickness range of about twenty layers where the iron grew in the fcc structure. (The SMOKE geometry used detects ferromagnetism parallel to the surface.) At greater iron thicknesses, when the structure reverts to bcc, we detect the presence of ferromagnetism through the occurrence of SMOKE intensity. Furthermore, the absence of detectable exchange splitting in the energy distribution curves (EDC's) in angular integrated ultraviolet photoemission (UPS) measurements is consistent with the absence of <u>any</u> magnetic ordering. The UPS results (using HeI radiation, 21.2 eV) at room temperature are shown in Figure 1 as a function of iron coverage.[5]

We have carried out fully-warped all-electron self-consistent Film Linearized Muffin-Tin Orbital (FLMTO) electronic structure calculations[7] for five layers of (100) fcc iron using the Cu lattice constant. The calculations are for both paramagnetic and spin-polarized states using 28 k-points in the irreducible 1/8 of the Brillouin Zone. The calculated density of states (DOS) in the different layers of the five-layer paramagnetic (100)fcc iron slab (solid curves), as well as for a five-layer slab of paramagnetic bcc iron (dashed curves), are shown in Fig. 2.

The UPS EDC's (see Figure 1) show markedly different features from those[8] of bcc iron. The EDC's show peaks at -1.1 and -3.2 eV for iron coverages of 3 to 10 layers. The 3.2 eV peak is clearly due to Cu, and as expected, diminishes and broadens with iron coverage. In marked contrast, the feature at 1.1 eV below E_F is seen to grow sharply with higher Fe

coverages. This feature is not due to surface states; no significant changes in peak intensity or position after O_2 and CO exposures were observed. This 1.1 eV peak is characteristic of fcc iron having approximately the same lattice constant as fcc Cu. Our calculated fcc Fe sphere-projected density of states (DOS) curves in Figure 2 show a sharp peak located quite close to the same energy, and this DOS peak is sharpest in the center layer. Kubler's[9] calculated bulk fcc Fe DOS has a peak at a slightly lower energy than our result, but we believe it is the same feature. Neither the experimental[8] EDC's nor the calculated[7] DOS of bcc iron shows any sharp features around 1.1 eV below E_F. (The weak feature at 6 eV below E_F in Figure 1, observed for thicker films, is probably associated with traces of oxygen on the surface.)

The calculated work function for the paramagnetic fcc iron slab of Figure 2 is 5.3 eV. Our earlier calculated results[7] for (100) paramagnetic bcc iron and for (100) fcc copper were 4.8 and 4.9 eV respectively. We have also calculated the electronic structure for a spin-polarized 5-layer fcc iron slab. The work function predicted for the magnetically ordered state is lower, 5.1 eV. (Our calculated work function for ferromagnetic bcc Fe(100) is 4.6 eV.)

Experimentally, an increase in the room temperature work function (determined from the width of the EDC's) of fcc iron is observed as compared to Cu(100), consistent with the predictions of the calculations for paramagnetic fcc iron. We measure a work function of 5.5±0.1 eV for one monolayer of iron. (For Cu (100) the work function is between 4.6 and 4.7 eV). The value for 0.5 monolayer of iron on Cu(100) is 5.3±0.1 eV; while for more than a monolayer the value remains around 5.4 eV. Our calculated electron-density maps help explain the work-function change when an Fe monolayer is put on the Cu substrate. The Fe orbitals which are

less spatially localized compared to Cu, and the stretched, near-surface Cu orbitals strengthen the surface dipole barrier, giving rise to the increase in the work function.

There is an indication of the presence of small splitting of the d-bands of about 0.5 eV at the as-deposited temperature 460K (inset in Fig. 1), in contrast to the lack of such features at room temperature.[11] The splitting disappears on cooling to lower temperature (shown for cooling to 320K in the inset to Fig. 1) and does not return upon heating back to 460K. The appearance of this feature was observed reproducibly in numerous experiments. (By itself it does not provide conclusive evidence of ferromagnetism. Such conclusive evidence is provided by SMOKE measurements.) The work function at 460K for a freshly grown film is 4.9-5.0 eV, a decrease from its room temperature value. This is in close agreement with our calculated value for the magnetically ordered state of fcc iron; however, one should bear in mind that the work function is, in any case, normally expected to decrease with increasing temperature. The presence of ferromagnetism in the as-grown 460K fcc iron-on-(100) copper was unequivocally identified by SMOKE measurements as shown in the upper and middle panels of Fig. 3. There is well defined hysteresis[10] at 460K as opposed to the absence of hysteresis at lower temperatures such as 300K, as shown in the lower panel of Fig. 3. As the temperature is lowered, say to 370K, the SMOKE signal abruptly disappears and does not return when the sample is reheated to 460K. The Auger spectra before and after the runs at 460K do not show any increase in contaminants during and after cooling to room temperature.

The interplanar spacing behavior as found by LEED is quite unusual. The LEED measurements involve intensity vs energy (I-E) determination on 13 spots. Multiple relaxation of the top three layers was allowed. For five

layers of Fe on Cu(100) at room temperature we find an interplanar distance of 1.81Å for the top layer compared to 1.78Å for fcc iron within the bulk, i.e. a surface interplanar expansion of about 1 or 2%. At 460K, the surface interplanar spacing further increases to 1.83Å, an expansion of an additional 1%. The intraplanar spacing remains equal to that of the Cu substrate.

There is strong evidence that the ferromagnetism at 460K is confined to the surface fcc iron layer. When the SMOKE intensity disappears with time,[10] the SMOKE signal can be restored by fresh deposit of a single layer of iron. Furthermore, the SMOKE intensity does not vary with fcc iron thickness and corresponds to a monolayer-type signal level when compared to previous bcc Fe-on-Au SMOKE measurements.[6]

It is interesting to consider this evidence for surface-only ferromagnetism in relationship to the results of our spin-polarized self-consistent LMTO calculations for a five-layer slab of fcc iron. The spin-polarized fcc iron calculation was started using the self-consistent paramagnetic potential with an artificial spin polarization favoring ferromagnetic coupling between all layers. However the final self-consistent result shows ferromagnetic alignment between the surface ($2.79\mu_B$) and subsurface ($2.30\mu_B$) moments, but the center layer moment ($1.68\mu_B$) is aligned antiferromagnetically to the subsurface moment. This would indicate surface ferromagnetism coupled to bulk antiferromagnetism. The total energy for the magnetically-ordered state is about 0.100 Ry below that for the paramagnetic state (out of some 12,705 Ry).

In conclusion, the results reported above show that fcc iron as grown on (100) copper "chooses" between two states that lie close in energy. Both states show an unusual interplanar expansion at the surface. The work function increase relative to copper observed for the lower-energy state

(State L) and the photoemission evidence for decreased or vanishing exchange splitting suggests that state L is paramagnetic, rather than ferromagnetic with alignment perpendicular to the surface. If this is so, either there is a transition at lower temperature to the theoretically-predicted magnetically-ordered ground state, or having such a paramagnetic state as the experimental ground state would contradict the results of our zero temperature total energy calculations (based on the local spin-density approximation). While the present calculations are for uniform interplanar spacing, one would expect expanded surface spacing to favor the magnetically -ordered state even more.[12,13] The surface layer in the higher-energy state (State H) is ferromagnetic parallel to the surface. There is strong evidence that the thermal transition from state H to state L is first-order. This is shown by the abrupt disappearance of the SMOKE signal on cooling, the failure to restore the ferromagnetism after cooling by cycling back up in temperature, and the ability to restore the ferromagnetism by deposition of iron at elevated temperature. The time decay[10] of the SMOKE intensity and of the exchange splitting provides evidence that state H, which is observed under as-grown conditions at 460K, is <u>metastable</u> with respect to state L at that temperature. This could be characteristic of a metastable situation created by growth conditions, e.g. by growth-induced strains which relax in time. For bulk ferromagnetic fcc iron, theory has predicted[12-14] a low moment to high moment transition with increasing volume. Moruzzi[13] has emphasized that the moment cannot show a gradual decrease to zero moment with decreasing volume. This would be consistent with great magnetic sensitivity to growth-induced strains, which may be strongly modifying the surface magnetic moment in magnitude and/or preferred alignment direction.

Acknowledgments: This research has been supported by the U. S. Department of Energy and the West Virginia University Energy Research Center. H. M. Naik was supported in part by a Research Grant from AMOCO. We are indebted to the Center for Materials Science at Los Alamos National Laboratory for supplying time on a Cray 1 computer. The work at Argonne was supported by U.S. DOE, BES-Materials Science under contract W-31-109-ENG-38.

References

1. U. Gradmann and P. Tillmanns, Phys. Stat. Sol. (a) 44, 539 (1977).

2. W. Wiartolla, W. Becker, W. Keune, and H. D. Pfannes, J. de Physique 45, C5-461 (1984).

3. A. Amiri Hezaveh, G. Jennings, D. Pescia, R. F. Willis, K. Prince, M. Surman, and A. Bradshaw, Solid State Commun. 57, 329 (1986).

4. M. F. Onellion, C. L. Fu, M. A. Thompson, J. L. Erskine, and A. J. Freeman, Phys. Rev. B33 7322 (1986).

5. Sample preparation and characterization was as described in Y. C. Lee, H. Min and P. A. Montano, Surface Science 166, 391 (1986).

6. S. D. Bader, E. R. Moog, and P. Grunberg, J. Mag. Magn. Mater. 53, L295 (1986)

7. G. W. Fernando, B. R. Cooper, M. V. Ramana, H. Krakauer, and C. Q. Ma, Phys. Rev. Lett. 56, 2299 (1986); C. Q. Ma, M. V. Ramana, B. R. Cooper, and H. Krakauer, Phys. Rev. B34, 3854 (1986).

8. L. G. Peterson, R. Melander, D. P. Spears, and S. B. M. Hagstrom, Phys. Rev. B14, 4177 (1976).

9. J. Kubler, Phys. Lett. 81A, 81 (1981).

10. The splitting is a transient phenomenon, disappearing in a period of about one hour. The SMOKE experiments also show the transient effect; the hysteresis indicative of ferromagnetism disappears in about one hour.

11. Refs. 3 and 4 both report angle resolved photoemission for Fe on Cu(100). They differ as to the evidence for exchange splitting and hence ferromagnetism at room temperature. Ref. 4 reports ferromagnetism and Ref. 3 reports no ferromagnetism is present.

12. C. S. Wang, B. M. Klein, and H. Krakauer, Phys. Rev. Lett. 54, 1852 (1985).

13. V. L. Moruzzi, Phys. Rev. Lett. 57, 2211 (1986); V. L. Moruzzi, P. M. Marcus, K. Schwarz, and P. Mohn, Phys. Rev. B34, 1784 (1986).

14. O. K. Andersen, J. Madsen, U. K. Poulsen, O. Jepsen, and J. Kollar, Physica 86-88B, 249 (1977).

Figure Captions

Fig. 1. Electron distribution curves (EDC's) showing relative number of electrons emitted (in arbitrary units, A.U.) as a function of energy (in eV), relative to the Fermi energy, for iron on copper (100). The numbers indicate the number of monolayers (ML) of iron on copper (100). (Inset) Energy distribution curves (EDC's) for 5 layers of fcc iron on Cu(100) at 460K (top) and after cooling to 320K (bottom).

Fig. 2. Comparison of sphere-projected density of states (DOS) for paramagnetic fcc (solid curves) and bcc (dashed curves) iron: (solid curves) Sphere-projected density of states (DOS) for a system consisting of a five-layer (100) slab of paramagnetic fcc Fe. The lattice constant has been taken as that of Cu. These curves have been smoothed by a Gaussian of full width at half maximum (FWHM) of 0.3 eV. The calculated work function for this system is 5.3 eV. (dashed curves) DOS of a five-layer (100) slab of paramagnetic bcc Fe. The calculated work function for this system is 4.8 eV.

Fig. 3. (a) SMOKE ferromagnetic hysteresis loop at 460K from 3 layers of Fe-on-(100)Cu grown at 460K; (b) average of eleven hysteresis loops on different runs from Fe films 2 and 3 layers thick, grown at 420K or 460K and measured at $\geq$360C. As shown in (c) the ferromagnetism disappears irreversibly upon cooling or after about an hour. (c) shows the eleven scans averaged after the ferromagnetism has disappeared.

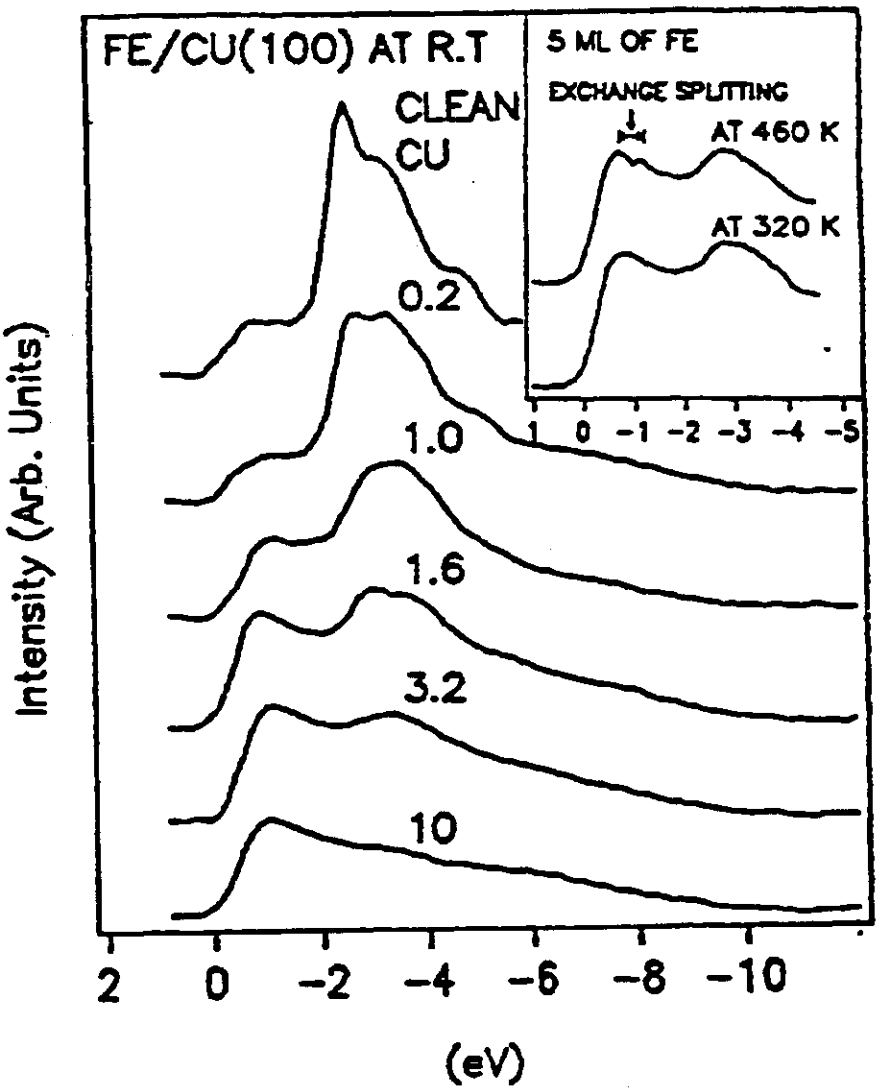
FE/CU(100) AT R.T
CLEAN CU
0.2
1.0
1.6
3.2
10
5 ML OF FE
EXCHANGE SPLITTING
AT 460 K
AT 320 K
1 0 -1 -2 -3 -4 -5
Intensity (Arb. Units)
2 0 -2 -4 -6 -8 -10
(eV)

Fig. 1

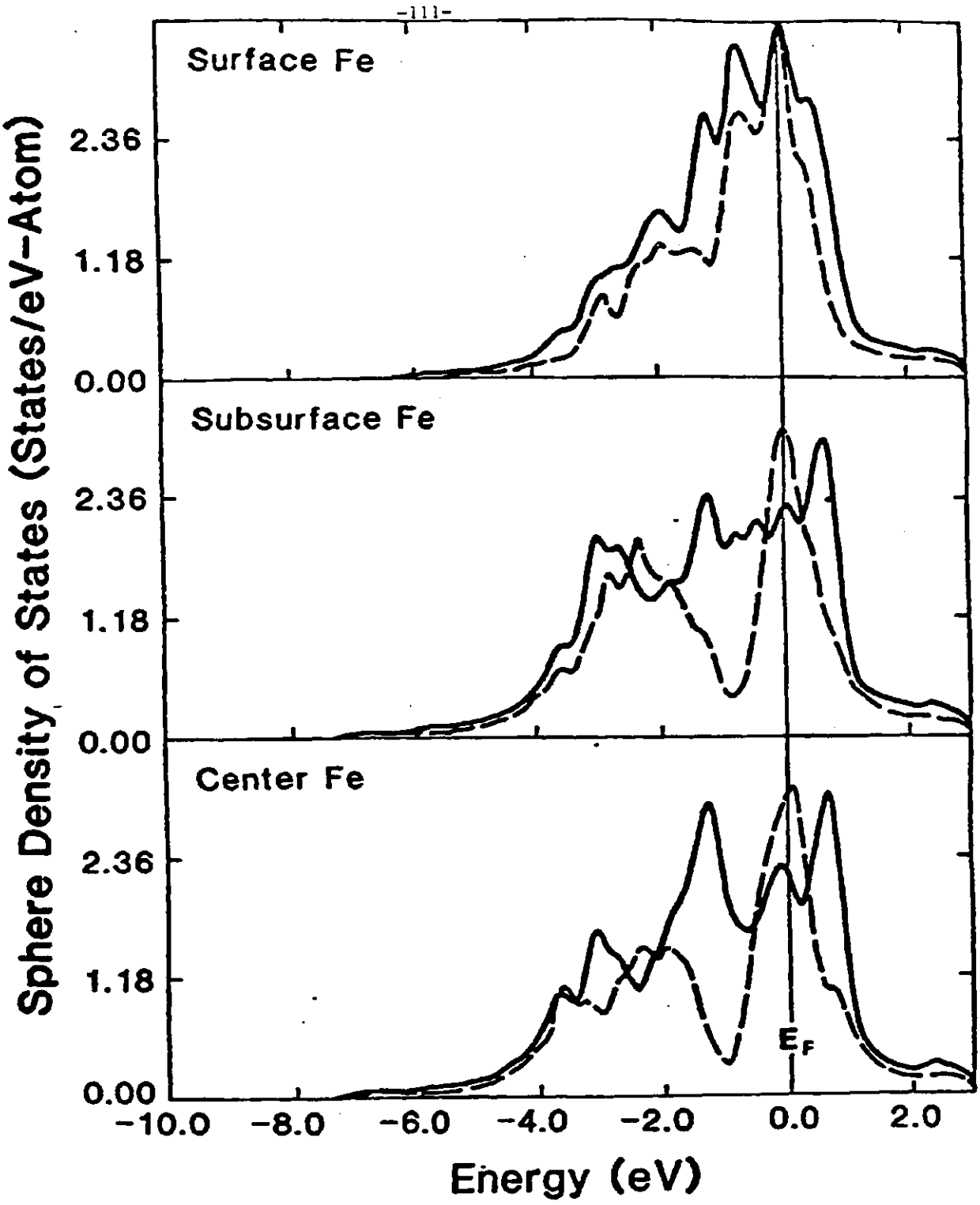
Surface Fe
Subsurface Fe
Center Fe
Sphere Density of States (States/eV-Atom)
2.36
1.18
0.00
E_F
-10.0
-8.0
-6.0
-4.0
-2.0
0.0
2.0
Energy (eV)

Fig. 2

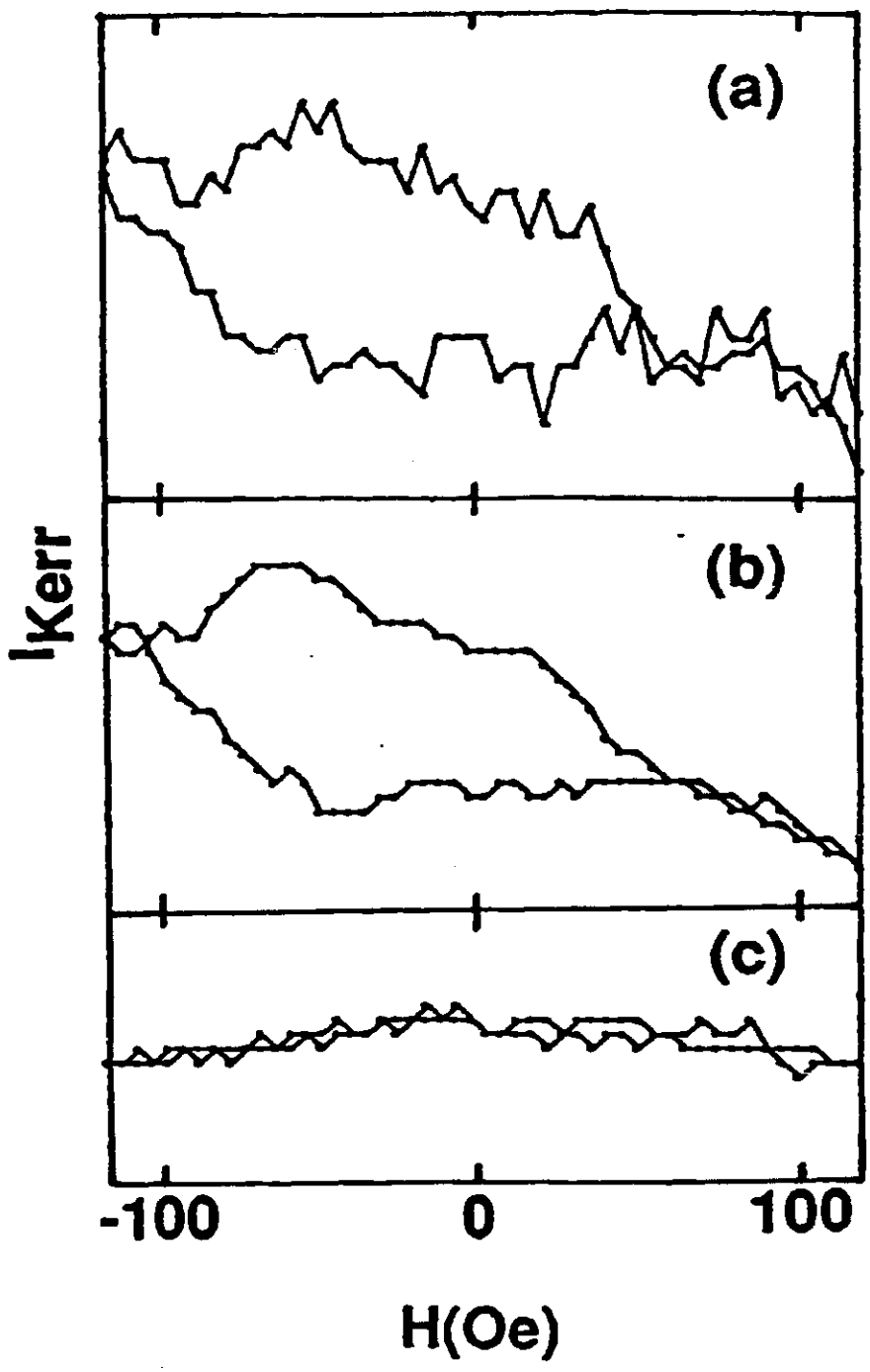

Fig. 3

6. AN ELECTRON ENERGY LOSS STUDY OF THE EPITAXIAL GROWTH OF IRON ON Cu(100)

(Quarterly Report January 16, 1987 - April 15, 1987)

Abstract

Iron was deposited under ultrahigh vacuum conditions on a clean Cu(100) surface followed by observation of the LEED patterns and EELS measurements. The LEED patterns showed a (1X1) structure with iron deposition indicative of epitaxial growth. Considerable changes in electron energy loss structures were observed with iron coverage. For low Fe coverages (<3 ML) the electron energy loss peaks of Cu(100) are distinguishable although there may be diminution in intensities and/or increase in peak widths. For higher Fe coverages, new loss features were observed. They can be associated with the f.c.c. γ-Fe film. For a thick layer of Fe on Cu(100), the spectrum is very similar to that observed for b.c.c. α-Fe.

1. INTRODUCTION

The epitaxial growth of one metal on another is of considerable importance in understanding the electronic structure of bimetallic systems known to differ significantly from that of bulk materials. The difference in electronic structure and modification in surface structure (e.g. f.c.c. iron on Cu(100)) may affect the catalytic properties and have implications in the tailoring of new catalysts in the synthetic fuel industry.

In this paper we report the results of measurements of iron deposited on Cu(100). LEED was used to characterize the surface geometry for all deposited iron. Auger spectroscopy was used to examine surface cleanliness and determine the surface composition after iron deposition. Electron Energy Loss Spectroscopy (EELS) in the reflection mode was used to obtain information about the electronic structure of the Cu(100)/Fe system.

2. EXPERIMENTAL

The experiments were performed in a UHV system with a base pressure of $2X10^{-10}$ torr. The system was provided with a CMA, 4-grid LEED optics, iron deposition source (tantalum Knudsen cell with a graphite boat) and a quadrupole mass spectrometer. In later runs the graphite boat was replaced by an alumina boat since it was found that cleaner samples can be prepared using alumina. The CMA was used for both Auger and EELS measurements. The LEED optics was used to observe the diffraction patterns for various iron coverages.

For EELS measurements, the negative second derivative of the electron distribution ($-d^2N/dE^2$) was taken by the lock-in differentiation technique. A modulation voltage of 1 eV was applied to the outer cylinder of the CMA.

A high purity Cu(100) disc was used for the measurements. The crystal

direction was verified by the von Laue X-ray back diffraction technique. Mechanical polishing followed by chemical etching produced a clean surface with a bright mirror finish. The Cu(100) crystal was mounted on the sample holder of the manipulator with a chromel-alumel thermocouple spotwelded to the side of the sample. In vacuum, the crystal was cleaned by alternate cycles of argon ion sputtering and heating until no surface impurities were detected with Auger spectroscopy (Figure 1a). A final annealing at 450°C for 5 min produced a clean surface with a sharp (1X1) LEED pattern.

Iron was deposited in increasing amounts on the Cu(100) surface while the growth of the 651 eV iron Auger peak and the diminution of the 920 eV copper Auger peak were monitored with deposition time. During the measurements, the iron deposition source was left on to maintain a constant deposition rate. The sample was rotated to face the evaporator and the CMA alternately. The iron source was interrupted by a shutter when an Auger measurement was made. LEED and EELS measurements were made in separate runs for different iron coverages.

With deposition of iron, small amounts of carbon and oxygen contaminants (~0.1 ML) were observed (Figure 1b, c), especially after long deposition time.

3. RESULTS AND DISCUSSION

3.1. Auger intensity versus deposition time and low energy Auger spectra -

The variation in intensity of the 651 eV iron Auger peak and the 920 eV copper Auger peak with deposition time is plotted in Figure 2. Initially the intensity of the iron Auger peak increases rapidly with iron coverage; at higher iron coverages, the rate of increase is diminished. The rate of decrease of the copper Auger peak follows a similar trend.

For a layer-by-layer growth, in a continuum approximation, the intensity of the copper substrate peak, I_{Cu}, would decrease according to the equation